Experimental determination of the phase-transition critical exponents α and η by integrating methods

C. Voges and H. Pfnür
Institut für Festkörperphysik, Universität Hannover Appelstrasse 2, D-30167 Hannover, Germany
(Received 14 August 1997)

Integrating methods in low-energy electron diffraction—turning the instrument to low resolution in $k_\parallel$—can reliably be used to study critical properties of continuous two-dimensional phase transitions and to determine critical exponents α and η. We performed systematic tests of the conditions under which an energylike power dependence of the diffracted intensity of superstructure beams can be observed in order-disorder phase transitions of adsorbed atomic layers belonging to three- and four-state Potts universality classes. As experimental examples, we studied the systems $p(2\times2)$- and $(\sqrt{3}\times\sqrt{3})R30°$-S/Ru(0001) and (2×2)-2H/Ni(111). We show that above T_c the condition for an energylike singularity, $K_I\xi\gg1$ (K_I: radius of integration in k space, ξ: correlation length) is already reached at $K_I\xi>3$, whereas below T_c effective exponents α are already obtained for $K_I\xi<1$. Therefore, in the temperature range below T_c this method to determine α turns out to be particularly easy to apply, and we concentrate on the determination of α below T_c in this study. Values of α of 0.67 ± 0.04 and 0.40 ± 0.05 were obtained for four-state Potts and three-state Potts systems, respectively. The latter value indicates small crossover effects to the critical behavior of the peak intensity. These studies were then further extended to the order-disorder transition of $p(2\times2)$-O/Ni(111), which is weakly first order, and to the effects of oxygen impurities in the system (2×2)-2H/Ni(111). We further show that in the limit $k\xi\gg1$ the exponent η can be determined from the $k_\parallel$ dependence of integrated ring intensities around positions of superstructure beams. With the systems mentioned, we demonstrate that the limit of a leading term of critical scattering which is independent of temperature can be reached by carrying out measurements going through the order-disorder phase transitions. Values of η of 0.27 ± 0.10 and of 0.30 ± 0.10 were obtained for the four-state and the three-state Potts systems, in close agreement with theoretical expectations. [S0163-1829(98)06206-7]

I. INTRODUCTION

The critical properties of continuous phase transitions in two dimensions (2D) for pure[1–3] and partially disordered or diluted systems[4] have attracted much interest in the recent past. This interest stems from the fact that due to the much larger influence of fluctuations in 2D compared to three-dimensional systems large deviations from mean-field behavior are expected and have been observed in several different universality classes both theoretically and experimentally.[1,3] From our own experience, strongly chemisorbed atomic adsorbates at concentrations of submonolayers on metal surfaces represent very good model systems for such studies.[5–8] Their continuous order-disorder phase transitions of commensurate phases give access to a variety of different universality classes in 2D, which would mostly not be accessible by magnetic systems.

Since fluctuations occur on all length scales at a continuous phase transition, an instrument which is only sensitive to short-range correlations and which integrates effectively over all long-range correlations, will also be able to measure critical properties. In the limit that the integration radius, k_I, around a superstructure beam fulfills the condition $k_I\xi\gg1$, these averages are predicted to have the same critical properties as the *energy*,[9] i.e., they should be proportional to $t^{1-\alpha}$ close to the critical point, where t is the reduced temperature t $[t=(T-T_c)/T_c]$. There have been some attempts both in experiment[7,10,11] and in simulations[12] to prove this prediction for order-disorder phase transitions in two-dimensional layers. However, the results were all more or less inconclusive, since none of them showed pure power-law behavior and partly large deviations from the expected exponents of known universality classes, although the deviations from power-law behavior were always found to be smaller below T_c than above. The origin of these deviations has never become clear, since no systematic tests of the conditions under which this power law can be observed, have been carried out in the past. These tests can only be done by experiment or simulation. If the determination of α would work reliably under well defined conditions, it would provide an easy experimental test of the nature of a given phase transition, and an easy discrimination between various universality classes, since the differences in α between different universality classes are the largest compared with other critical exponents.

The use of integrated low-energy electron-diffraction (LEED) intensities for determinations of critical properties is not limited to the determination of the exponent α. It is well known[13] that in the limit $k_\parallel\xi\to\infty$ critical scattering has a leading term

$$\chi(k_\parallel,t)=C\xi^{\gamma/\nu}D_\pm=A_\pm k_\parallel^{-(2-\eta)}(1+\cdots), \qquad (1)$$

which is independent of temperature. If this limit can be reached experimentally, a determination of the critical the exponent η, the anomalous critical dimension, is easily possible from integrating the intensity in a ring around a superstructure spot:

$$R_I = 2\pi \int_{k_1}^{k_2} k\,dk\,I(k) \approx A_{\pm} \frac{\pi}{1-\eta}(k_2^{\eta} - k_1^{\eta}), \qquad (2)$$

thereby avoiding any contribution from long-range order, which is centered at the Bragg position.

While the exponent η, is temperature dependent for dislocation induced transitions,[14,15] it remains constant for order-disorder phase transitions. If the method described above works, it would not be limited to the case of constant η, and would thus be generally applicable. Only the former case, however, has been tested by profile analysis in x-ray scattering.[16]

In this paper, we give an overview over a systematic study of the experimental feasibility to determine the critical exponents α and η from integrating intensities of LEED. By systematic variation of the radii of integration around two-dimensional superstructure Bragg positions, we show in this paper that the limit $k_{\parallel}\xi \gg 1$ is reached rather easily, so that the critical exponents α and η can be determined reliably from integrating methods with LEED. We have performed these tests with the atomic adsorbates H and S on Ni(111) and Ru(0001) surfaces, respectively, for average concentrations below 0.5 monolayer (ML). Particularly the system H/Ni(111) represents a crucial test system due to its small scattering amplitude. The order-disorder phase transitions of the (2×2) phases on both surfaces have been shown to be continuous and to belong to the four-state Potts universality class,[7,17] whereas the transition of the $\sqrt{3}\times\sqrt{3}R30°$ structure belongs to the three-state Potts class.[7] A short preliminary version of parts of these studies has been published recently.[18]

II. EXPERIMENTAL PROCEDURES

Experiments were carried out in a μ-metal shielded UHV chamber (base pressure of 3×10^{-11} mbar) pumped by titanium sublimation and turbo molecular pumps. LEED intensities were measured using a conventional backview LEED optics.

The samples (10 mm in diameter, 1.5 mm thick) were cut by spark erosion from single crystal rods, etched, precision oriented to better than 0.2°, and polished with diamond pastes down to 0.25 μm grain size. After extensive sputtering/annealing cycles for Ni (heating/cooling cycles in 5×10^{-7} mbar oxygen for Ru), no contaminants were detectable any more with Auger spectroscopy long before these cycles were completed. From high-resolution LEED profile measurements of integral order spots as a function of electron energy on the clean surfaces an average step width of 300–400 Å was deduced, which were separated by monoatomic steps.

Order-disorder phase transitions of chemisorbates have to be measured at constant coverage. Since under these conditions, critical exponents at an arbitrary point in the phase diagrams are Fisher renormalized[19] and therefore hard to extract, our measurements were always carried out at points with maximal T_c, where $d\mu/d\Theta = 0$, so that renormalization is suppressed. These symmetry points in the phase diagrams always corresponded to the perfect completion of the respective superstructures, since the maximum of superstructure spot intensity coincided with the maximum transition temperature in all cases investigated. All our measurements were taken at respective maximum intensities of the superstructure spots under consideration.

All gases were dosed on the sample via background pressure at a crystal temperature of 250 K for H, and of 400 K for H_2S, which on Ru immediately dissociates to form atomic S, and for O_2. During exposure the superstructure spot intensity was recorded versus time. At maximum intensity of the superstructure spots, the exposition was stopped. After one annealing cycle at higher temperature, the the spot intensity I was monitored versus temperature while cooling down, which allowed a second check of the coverage by determining the critical temperature from the inflection point of the $I(T)$ curve (see below). This measurement was repeated routinely in short intervals to make sure that T_c has not shifted by adsorption of background gas, etc. In the experiments in which small amounts of oxygen were used as impurities in a hydrogen layer on Ni(111), we used a capillary array and a pneumatic valve, which allowed a reproducibility of 0.5%.

Whole images of approximately one substrate Brillouin zone (BZ) were taken with a cooled slow scan CCD camera (512×512 pixels with 14 bit resolution) and stored on a personal computer. The variation of the integration radii, background subtraction, etc. was done afterwards on the digitized images stored on the computer. By use of ℓN_2 and resistive heating through the crystal mount or electron bombardment the sample temperature could be varied between 100 and 1400 K. Only resistive heating (alternating current at 20 kHz with trapezoidal envelope at 25 Hz) was used for the measurements. The LEED beam was turned on only in the time intervals with zero heating current. Temperature was measured with a resolution of 0.01 K using a NiCr-Ni thermocouple—WRe5%-WRe26% in the case of Ru—spot welded to the rim of the sample. A computerized feedback circuit stabilized the sample temperature to ± 0.02 K.

III. DETERMINATION OF THE CRITICAL EXPONENT α

A. Debye-Waller factor and thermal diffuse background

Integration of diffracted intensities is quite sensitive to background, which has to be subtracted. Background can be either elastic or inelastic within the typical resolution of a LEED experiment (1–3 eV). Both its temperature and its $k_{\parallel}$ dependence is of interest here. Background induced by static disorder, however, which is present in all systems investigated here, has no temperature dependence. Although not explicitly tested, we assumed that the defects were uncorrelated so that no $k_{\parallel}$ dependence is expected either. A further component is inelastic background due to low-lying electronic excitations. Only the $k_{\parallel}$ dependence could cause ambiguities, which, however, concluding from the results below, seems to be small enough for all cases tested that it can be neglected for the present measurement.

Therefore, we concentrate on thermal diffuse scattering, which influences both peak and background intensities. The peak intensity itself—only superstructure spots are of interest

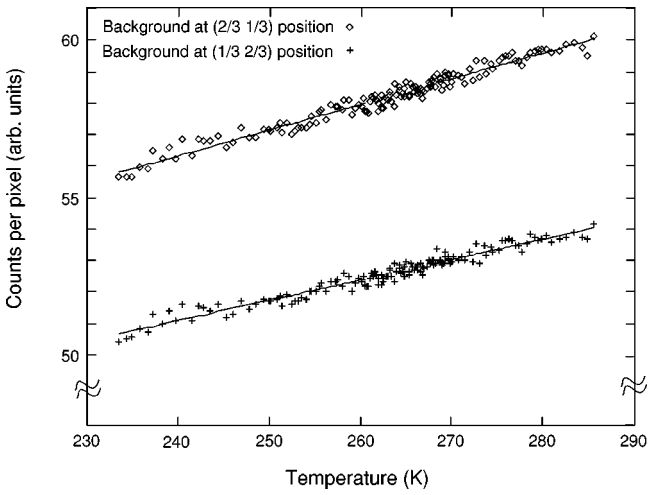

FIG. 1. Temperature dependence of the background intensity of (2×2)-2H, integrated over a circle of 6% BZ radius, centered at K_1 and K_2 points of the surface Brillouin zone. Intensity increases linearly with temperature as indicated by the straight line. For details of the temperature dependence see text.

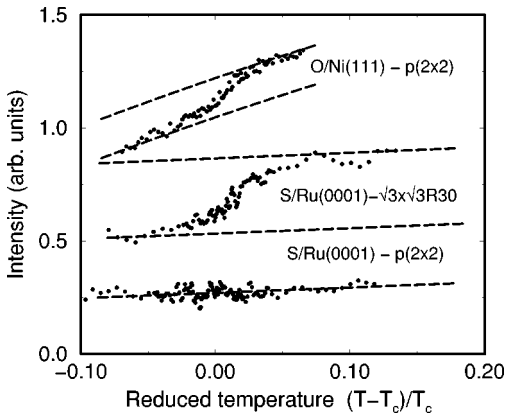

FIG. 2. Temperature dependence of the background intensity of the systems S/Ru(0001)-$p(2\times2)$ and -$(\sqrt{3}\times\sqrt{3})R30°$, and of O/Ni(111)-$p(2\times2)$, showing a characteristic increase due to uncorrelated site changes close to the respective order-disorder phase transitions. The dashed lines correspond to the increase due to thermal diffuse scattering alone. Curves have been shifted for clarity.

here—decreases with increasing temperature due to vibrations of adsorbate and substrate atoms. This effect can be taken into account by a Debye-Waller correction, $\exp(-2MT)$, assuming uncorrelated and isotropic motion of the surface atoms as a first approximation, whereby the factor $2M$ is determined experimentally. This approach describes the decay of peak intensities satisfactorily in most cases. Care must be taken, however, in cases with thermally activated changes of sites. There, this approach is only valid at low enough temperatures. A corresponding additional decrease of peak intensities and a contribution to the background far away from the Bragg spots was seen (see below).

The background far away from Bragg positions induced by thermal diffuse scattering is dominated at higher temperatures by multiphonon processes, as experimentally shown.[20] In this limit, the thermal diffuse background is independent of the scattering vector and can be described within the approximations just mentioned by a $1-\exp(-2MT)$ behavior.

The one-phonon contribution, if excited by dipole scattering, has a $(\Delta k)^{-1}$ dependence, and leads to a broadening of the spot intensity. This contribution turns out to be small even on surfaces with low Debye temperatures like aluminium,[20] and can therefore only be resolved by an instrument with high angular resolution. We therefore expect that it will neither have a significant effect on the temperature dependence nor on the $k_\parallel$ dependence in our integrative measurements. This is in good agreement with our findings.

In order to determine the background, we measured the reflected intensity at distances as far away as possible from Bragg positions of the superstructure. As a first example, the background intensity of (2×2)-2H at 0.5 ML coverage at $k_\parallel$ positions $(\frac{1}{3},\frac{2}{3})$ and $(\frac{2}{3},\frac{1}{3})$ are shown in Fig. 1 as a function of temperature. A dark image was subtracted from these data, which was taken with the same exposure time and with an open focal plane shutter of the CCD camera. Only the electron beam of the LEED gun was suppressed. The thermal diffuse background was extracted at $k_\parallel$ positions exactly between the superstructure spots and averaged over a diameter of 12% of $|k_{10}|$ in the temperature range $\pm10\%$ around the phase transitions. Figure 1 shows a linear dependence on temperature. No additional increase of intensity above $T_c = 268.1$ K can be seen. This indicates that no site exchange of hydrogen to a third adsorption site takes place. Also, the relaxations of the nickel substrate can only be changed very little, since significant changes would lead to modified scattering factors, and would therefore cause an increase of background signal.

This linear increase can be described by use of the high-temperature expansion of the Debye model, neglecting anisotropic vibrational frequencies. In this model, the background intensity behaves like $|A|^2\{1-\exp(-2MT)\}$, with $M\propto(m\Theta_D^2)^{-1}$. Θ_D is the Debye temperature and m the mass of a vibrating atom. Since $MT<1$, this expression can be linearized $1-\exp(-2MT)=2MT+O(M^2T^2)$. If the background intensity is assumed to be pure thermal diffuse scattering, the constant M can be extracted by a straight line fit, from which we obtain a value $2M=0.0020\pm0.0002$ for $E=45$ eV and the $k_\parallel$ positions indicated in Fig. 1. Inserting for m the mass of a substrate atom, we obtain a Debye temperature of $\Theta_D=270\pm15$ K. This Debye temperature agrees very well with other measurements.[21–23] Two conclusions can be drawn from this result: First, hydrogen vibrations are not excited to an appreciable extent at these temperatures,[24] i.e., even at and above the disordering temperature. Second, the main contribution to the background intensity is indeed thermal diffuse scattering. For the measurements described below, this (averaged) experimentally determined background was subtracted from the data shown below without further adjustments.

The situation is significantly different in the systems O/Ni(111)-$p(2\times2)$ and S/Ru(0001)-$(\sqrt{3}\times\sqrt{3})R30°$, for which measurements have been taken in the same way as those described above. These data are shown in Fig. 2 together with the data for the $p(2\times2)$ structure of S/Ru(0001), which behaves very similar to the H/Ni(111) system discussed above. The measurements were carried out for the same radii of integration at the respective $\overline{K}$ and $\overline{M}$ points of the first Brillouin zone at energies of 64 and 67 eV for

S/Ru(0001) and at 90 eV of O/Ni(111). In the S/Ru(0001)-$p(2\times2)$ system again, the vibrations of the adsorbate itself do not contribute to the Debye-Waller effect, and the small increase of background intensity observed is compatible with vibrational excitations of only the substrate, which yielded $\Theta_D = 540$ K, in good agreement with the optimizations carried out in LEED-IV studies.[23] The data for the other two systems show that they are also compatible with this description far away from T_c (the larger slope for Ni is due to $\Theta_{D,Ni} = 270$ K), but close to T_c an S-like increase is seen. This increase is directly related to the thermally excited uncorrelated occupation of the second threefold site. A quantitative determination of the occupation probability of this site has been carried out recently by us.[25] Details are discussed there. Consistently, no occupation of the second threefold site has been found close to the phase transition in the S/Ru(0001)-$p(2\times2)$ system. Since this change of sites can consistently be described by an uncorrelated random process, no $k_\parallel$ dependence should be expected. Therefore, we again simply took this temperature-dependent background into account in our data evaluation described below by scaling these intensities appropriately according to the various radii of integration.

B. Determination of the critical exponent α below T_c

1. Determination of T_c

An instrument with finite resolution in $k_\parallel$ space is expected to effectively always integrate over critical fluctuations once a temperature sufficiently close to T_c is reached. Therefore, even for the peak intensity close to T_c scaling $\propto |t|^{1-\alpha}$ is expected, provided that the correlation length is not limited by the finite size of the system before this condition can be reached. Integration over a superstructure peak only widens the temperature range in which this condition is fulfilled. The derivative of these intensities with respect to temperature, I', should diverge $\propto |t|^{-\alpha}$ with the divergence at T_c. Since a real experiment is always carried out on systems of finite size—in the case of a LEED experiment it takes the average over a large number of finite-size subsystems—the divergence turns into a maximum. This maximum can be easily determined experimentally, and allows the best (experimentally) possible estimate of the critical temperature. From the width of the peak of I' an estimate of the uncertainty is also possible. For all examples shown below, T_c has been determined by this procedure, and no further adjustments of T_c were made.

As an example, the integrated superstructure spot intensity of the $(\frac{1}{2}0)$ of the H/Ni(111) system is plotted versus temperature in Fig. 3 for various radii of integration. These intensities have been obtained by summing up all pixel values of the CCD image lying within a circle of a given diameter. A dark image has been subtracted. The center of the circles had been carefully positioned at the superstructure spot to ensure correct integration even with small radii.

As expected, the maxima of I' do not shift as a function of the radius of integration, and even the shape of the curves is approximately constant for integration radii above 3%, as shown in the bottom part of Fig. 3. The maximum of these curves gives $T_c = 268.3$ K. From the rounding of the curves at the top we estimate an uncertainty in T_c of ± 0.5 K. This uncertainty turned out to be the main source of uncertainty in the determination of α. With T_c fixed as described, effective values of α were obtained from log-log plots of I' for various integration radii, k_I.

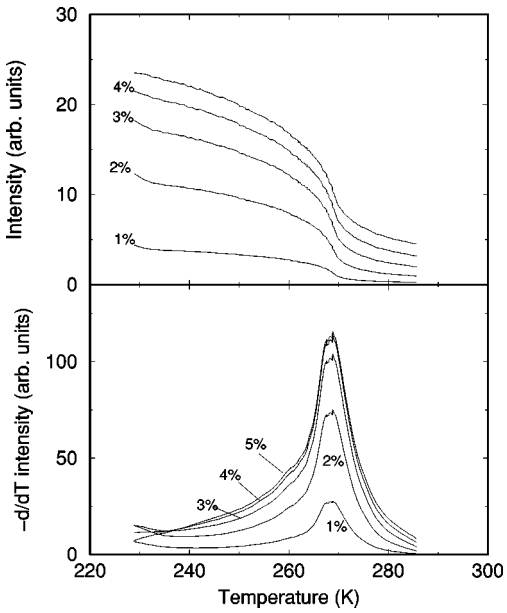

FIG. 3. Top: Temperature dependence of integrated intensities of the $(\frac{1}{2},0)$ superstructure spot in the system (2×2)-2H close to the order-disorder phase transition for various radii of integration (in units of the diameter of the substrate Brillouin zone). Bottom: Same intensities differentiated with respect to temperature. The critical temperature was determined by the maxima of these curves.

2. H/Ni(111)-(2×2) and S/Ru(0001)-p(2×2)

As already indicated in Fig. 3, the data above and below T_c are not symmetric. Therefore, we analyze them separately, and first discuss the data below T_c. Hydrogen due to its small signal is clearly the most crucial case. In Fig. 4 we show an extended set of data for I' in a log-log plot using T_c as describe above. A power-law behavior is seen over slightly less than one order of magnitude in t between 0.01

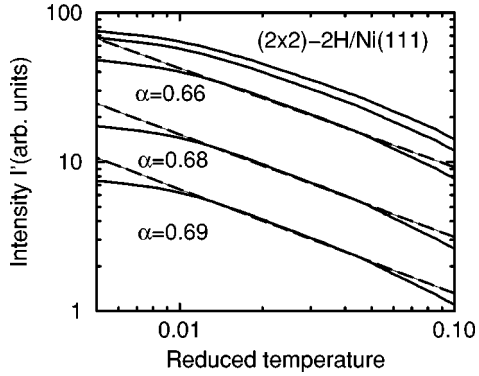

FIG. 4. Log-log plot of temperature derivatives, I', of integrated intensities of first-order superstructure beams as a function of reduced temperature for (2×2)-2H/Ni(111) below T_c. The radii of integration vary between 0.6% (lowest curve) and 4% (in units of $|k_{10}|$).

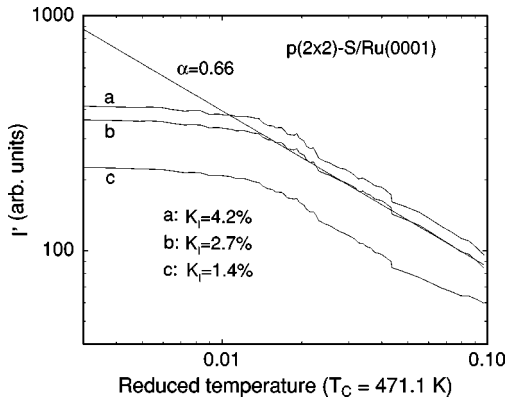

FIG. 5. Log-log plots of temperature derivatives of integrated intensities of superstructure beams as a function of reduced temperature for $p(2\times2)$ S/Ru(0001) below T_c, and for the radii of integration as indicated. The straight line corresponds to a power law with $\alpha=0.66$.

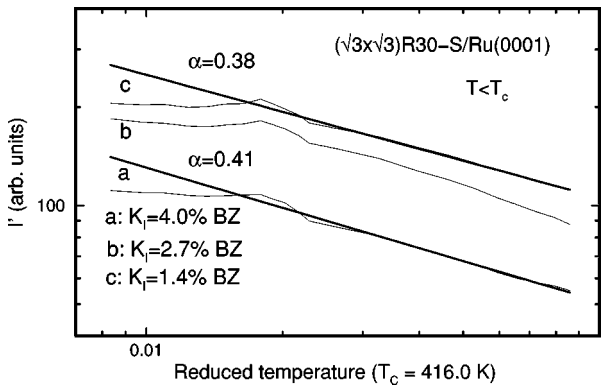

FIG. 6. Same as Fig. 5, but for S/Ru(0001)-$(\sqrt{3}\times\sqrt{3})R30°$.

and 0.1 for H/Ni(111). Remarkably, almost no dependence of either the slope or the range of power-law behavior on the integration radius was found. The integration radii, k_I, were varied between 0.6 and 4%. This range of integration radii is limited by the resolution of the LEED instrument at the low end, whereas for radii larger than 4% no significant variation of I' was found as a function of k_I.

The range in reduced temperature, on the other hand, is restricted by finite-size effects at small t. From a previous analysis of the critical exponents β, γ, and ν (see Ref. 17) the correlation lengths as a function of reduced temperature are known above T_c and found to be limited by the terrace length on the sample. On the Ni sample used for the present investigations the terraces were only about 300 Å wide. Combining these results, a crossover to finite-size limited behavior for $|t|\leq 0.01$ must be expected, in agreement with our findings. The deviation at large t can be due to slightly incorrect background subtraction. However, in order to keep the analysis free of adjustable parameters, we have not made any attempt to adjust the background. Another possibility is the occurrence of corrections to scaling, which due to their logarithmic character should be quite important for the four-state Potts universality class, to which this system is expected to belong.[26,17] If this is the reason for the deviations at large t, it would indeed be the first indication for corrections to scaling for a two-dimensional system in this universality class, according to our knowledge.

Indeed, an error in background subtraction at large t for the (2×2)-2H system seems to be more likely than corrections to scaling, since no indication of deviations from power-law behavior were found in the system $p(2\times2)$-S/Ru(0001), for which the analogous data are shown in Fig. 5. Here the signal is much higher than for H, so that the data are less sensitive to background subtraction. With roughly the same quality of crystal surface as for Ni(111), scaling is again observed over the same range of t. Similar to the H/Ni(111) system, very little sensitivity of the effective critical exponent α on the radius of integration is seen.

Although there is a slight tendency to smaller values with increasing k_I, which, however, is still within the limits of uncertainty, the values of the effective exponent α obtained in these two systems not only agree with each other, they also coincide almost perfectly with those of the expected four-state Potts universality class. From various data sets we obtain effective values of $\alpha=0.68\pm0.07$ for H/Ni(111) and of 0.66 ± 0.07 for S/Ru(0001)-$p(2\times2)$. The contributions to the error bars by the uncertainty in T_c and by the variations in slopes between different data sets are about equal. It is obvious that neither corrections to scaling nor the addition of nonsingular terms could improve our result. Therefore, logarithmic corrections expected in this universality class[26] do not seem to play an important role.

3. S/Ru(0001)-$(\sqrt{3}\times\sqrt{3})R30°$

Similar behavior in the same range of t is observed for I' on the $(\sqrt{3}\times\sqrt{3})R30°$-S/Ru(0001). The data below T_c are shown in a log-log plot in Fig. 6. They yield an effective exponent α of 0.40 ± 0.05. This value is slightly larger than expected for the three-state Potts universality class ($\alpha=\frac{1}{3}$), but any attempt to add additional terms to the simple power law only made the value of α more dependent on the integration radius, but did not systematically shift it closer to $\frac{1}{3}$. Again, a tendency towards smaller values of α is found with increasing radii of integration. This finding [to some extent also seen in the data of the (2×2) structures shown in the previous section] suggests that the reason for this discrepancy are influences of crossover to the behavior at small $k_\parallel\xi$ with an exponent $(1-2\beta)$, which is 0.78 and 0.83, for three and four-state Potts classes, respectively. Since α is much closer to $1-2\beta$ for the four-state Potts systems than for the three-state Potts system, this effect is much more severe in the latter case, in agreement with our observation. Corrections to scaling could play a role, but should be more prominent in four-state Potts systems than in three-state Potts systems due to the logarithmic terms in the former.[26] In agreement with our findings for the exponent α, these have been shown to have little influence in the determination of the exponents β, γ, and ν.[17,7,10]

We conclude, therefore, that even on our surfaces with relatively small terraces where scaling can only be observed at reduced temperatures $t>0.01$, a clear discrimination between different universality classes is possible from the integrated intensities below T_c. Even on these rather imperfect surfaces, the obtained effective values for α are only slightly influenced but not dominated by crossover to $(1-2\beta)$ behavior. This effect should be strongly reduced closer to T_c,

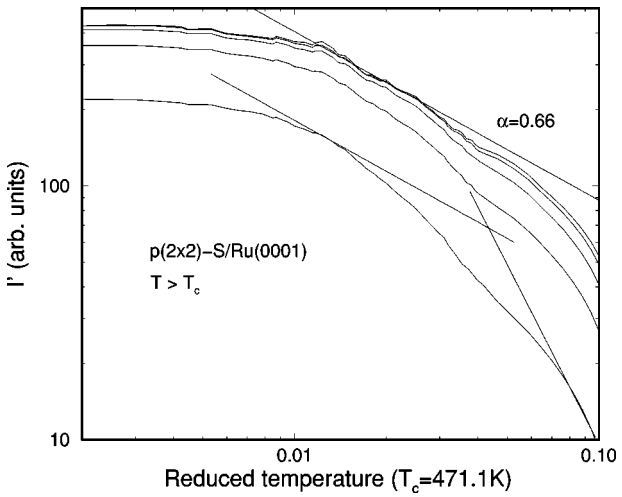

FIG. 7. Log-log plot of the derivatives of integrated intensities, I', above T_c for S/Ru(0001)-$p(2\times2)$ measured with the radii of integration (curves from bottom to top) $K_I=1.35$, 2.7, 4.0, 5.4, and 8.0% BZ. The straight lines in the middle correspond to the power-law behavior found below T_c ($\alpha=0.66$). The slope of the straight line drawn in the lower right corner corresponds to a slope of $-(\gamma+1)=-2.17$.

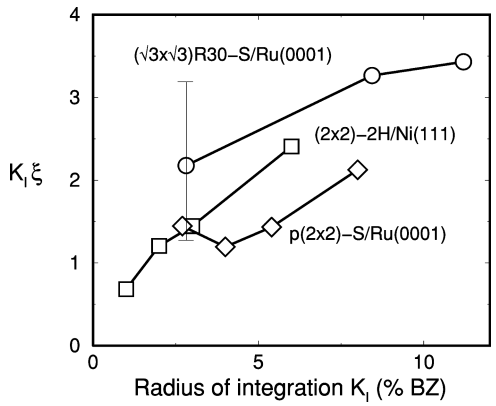

FIG. 8. Limiting values of $K_I\xi$ above which energylike behavior of integrated LEED intensities ($I\propto t^{1-\alpha}$) is found above T_c. For further details, see text.

for which, however, surfaces with much larger terraces are needed.

C. Determination of α above T_c

The good power-law fits have no direct correspondence above T_c. Above T_c none of the three systems investigated shows pure power-law behavior. As a typical example, the derivatives with respect to temperature of integrated intensities are shown in Fig. 7 for the system S/Ru(0001)-$p(2\times2)$, and for different integration radii. Whereas the flat region below $t=0.01$ has already been identified as being due to finite-size rounding, there are small sections of the curves with the largest radii of integration which decay with the expected power of $\alpha=0.66$. Reducing the radius of integration causes the range over which the curves can be fitted by this power law to shrink until, at a radius $K_I=1.35\%$ this range cannot be determined any more. In all cases, the range over which a power law can be fitted is too small to really determine an effective critical exponent. On the other hand, the reduction of the range of power-law behavior as a function of decreasing radius of integration agrees with the expectation that deviations from a power law should occur after the product $K_I\xi$ falls below a certain limit.

At large t, the condition $K_I\xi\gg1$ is clearly no longer fulfilled, and the slope should finally crossover to the behavior of the peak intensity (i.e., its derivative in our case) with a limiting slope in a log-log plot of $-(\gamma+1)$, which for the four-state Potts class has a value of -2.17. This slope is also drawn in Fig. 7, and is shown to agree well with the limiting slope close to $t=0.1$. Very similar behavior was found in the systems (2×2)-2H/Ni(111) and S/Ru(0001)-$(\sqrt{3}\times\sqrt{3})R30°$. These data show that the critical exponent α can, in principle, also be measured above T_c. Our data, however, also show the restrictions of this method above T_c. First, the radius of integration clearly limits the range where a power law can be observed, as generally expected. Second, in order to observe pure power-law behavior of integrated intensities above T_c over a reasonable range of t, i.e., at least over one order of magnitude in t, much higher requirements on the available length scales, i.e., on the terrace lengths of the sample surfaces for the cases studied here, are necessary.

The limited perfection of our samples, however, still allows an estimate of the limiting values of $k_\parallel\xi$ for the ''correct'' slope of α, using the known values of α and the correlation lengths determined from spot profile analysis as a function of t.[7,17] A plot of the values of $K_I\xi$ at the points where the deviations from the power laws with slope $-\alpha$ can first be observed, are shown for the three systems under investigation in Fig. 8. $k_\parallel\xi$ for the ''correct'' slope of α turns out to be between 1 and 2 for the (2×2) systems and around 3 for the $\sqrt{3}$ system.

D. Discussion

Our results presented so far seem to suggest that the limit $K_I\xi\gg1$ can indeed be reached experimentally. Above T_c it turns out that $K_I\xi$ only needs to be of order 1, i.e., between 2 and 3. As seen from the results above, with a maximum K_I of about 6% BZ, above which only the signal-to-background ratio goes down without gaining more information, correlation lengths $\xi>30a$ are necessary (a is the lattice constant). In order to obtain significant data, at least one order of magnitude in t is necessary. This requires extremely perfect surfaces with undistorted terraces of at least $300a$ or 1000 Å. Although such perfect surfaces can be produced, they are not available routinely.

To our surprise, the situation can be managed more easily below T_c. Here the condition $K_I\xi\gg1$ is obviously violated, but still an energylike singularity can be observed for the systems investigated, and under our conditions of measurements. From simulations for $p(2\times2)$ and $(\sqrt{3}\times\sqrt{3})R30°$ structures[9,12] an estimate of 4:1 for the ratio of correlation lengths above and below T_c at the same value of $|t|$ is obtained. Together with the absolute values of ξ obtained in these simulations above T_c, we can estimate that for the $p(2\times2)$-S/Ru(0001) structure, e.g., $K_I\xi$ is between 0.1 and 0.5 for $K_I=1.4\%$ BZ and the temperature range $0.01<|t|<0.1$. For the other systems the same order of magnitude is obtained.

This difference in the behavior above and below T_c must be attributed to the different form of the response function $D_\pm$ above and below T_c in the general scaling ansatz for critical scattering $\chi(k_\parallel,t)=C|t|^{\gamma}D_\pm(k_\parallel\xi)$. Unfortunately, these response functions $D_\pm$ are poorly characterized for the three- and four-state Potts models. Rough estimates have been obtained above T_c from expansions in $4-\epsilon$ dimensions.[27,28] For $T>T_c$ they show qualitatively[29] that our experimentally accessible range of reduced temperature above T_c is completely dominated by crossover between $t^{-\alpha}$- and $t^{-\gamma-1}$-behavior, in agreement with the experimental observation. Our results below T_c, however, have no theoretical correspondence, but should be used as input for further theoretical efforts.

As mentioned, detailed calculations about the feasibility of determining α from integrated diffracted intensities have been carried out by Bartelt *et al.*,[9,12] and it is worthwhile comparing these results from theoretical calculations and simulations with our experimental data. In agreement with these calculations, we find that a term linear in $|t|$ contained in the reponse function $D_\pm$ does not play an important role. This contribution as a function of K_I is proportional to $K_I^{\eta-1/\nu}$, i.e., it decreases with increasing K_I since $1/\nu>\eta$ for the universality classes considered here. Experimentally, we mention that we have subtracted out a linear increase of the thermal diffuse background. According to the calculations of Bartelt *et al.*,[9] however, the amplitude of the energylike singularity should depend on K_I like $K_I^{(1-\gamma)/\nu}$, i.e., the integrated intensities should depend on K_I like $I\propto K_I^{-0.5}$ and $I\propto K_I^{-0.25}$, respectively, for three- and four-state Potts systems. This reduction of the energylike singularity was not observed in experiment. In the range of K_I investigated the amplitude of the (pseudo-)singularity increased and finally leveled off, but did not decrease. The reason simply might be that we have not entered the range where the temperature-independent term dominates (see below).

E. The critical exponent α: more complicated systems

From the results presented above, the use of integrated intensities of superstructure beams to determine the critical exponent α (or to get at least a good estimate for it) seems to work reliably below T_c even on samples which have terrace widths of only 100 lattice constants. Based on these rather promising results, we tried to extend this method to more complicated systems and present two examples of them below.

The first is O/Ni(111)-$p(2\times2)$, the critical properties of which are still rather controversial, since the experiments of three different groups[30,22,31] yielded results which are incompatible with each other. Correspondingly, the interpretation of the data varies between continuous and weakly first order. The other example refers to the influence of oxygen impurities on the system H/Ni(111)-(2×2).

1. O/Ni(111)-p(2×2)

The crystal used for these experiments was cut from a different crystal rod than that used in previous experiments[32] and was supplied by a different manufacturer. We therefore expect that, even if there were some influence by impurities, it should be different on the various samples used. As mentioned, the surface had a terrace width of only 300 Å, which is much smaller than on the sample previously used for the determination of the exponents β,γ and ν,[22] but comparable to that in the experiment of Li *et al.*[31]

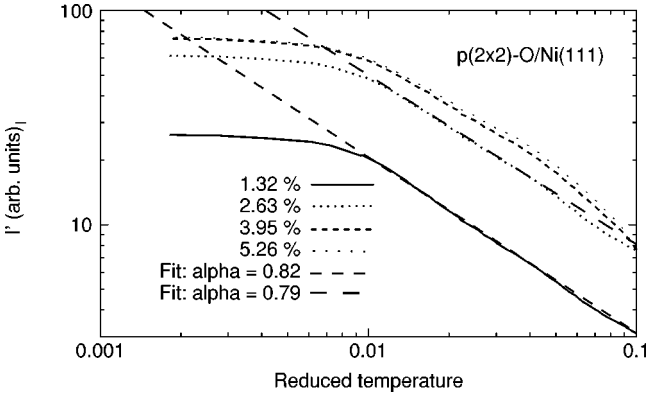

FIG. 9. Same as Fig. 5, but for O/Ni(111)-$p(2\times2)$.

Typical results for measurements below T_c are shown in Fig. 9 for various radii of integration. The raw data have been corrected by a Debye-Waller factor corresponding to a surface Debye temperature of 280 K, as determined above. Also the procedure to determine T_c was identical to that described above. Care was taken to avoid electron-induced effects. The change in peak intensity at a given temperature over the whole time of measurement was kept below 5%. Again power-law behavior was found in the range of reduced temperatures $0.01<|t|<0.1$, yielding an effective critical exponent $\alpha=0.80\pm0.04$. The error bar contains the scatter of several data sets and of various radii of integration, which were varied between 1 and 6% BZ. The leveling off at small reduced temperatures again occurs at comparable reduced temperatures, where in our profile analysis we found similar behavior for the correlation length.[22] In the present situation, the terrace length coincides with the value of the correlation length at the leveling off, whereas in our previous experiment we had much larger terraces, but leveling of the correlation length again at 300 Å.

This value of α is significantly larger than that obtained for the continuous phase transitions of the (2×2) structures of H/Ni(111) and of S/Ru(0001). It is actually between the values expected for a continuous transition in the four-state Potts class and a first-order phase transition, for which $\alpha=1$ is expected.[33] Interestingly, the hyperscaling relation $\alpha=2-2\nu$ is almost perfectly fulfilled, since we obtained $\nu=0.60$ in the previous measurements.[22]

This deviation from the critical exponents of the four-state Potts universality class cannot be accidental. The result obtained here and our previous results for the critical exponents β,γ, and ν, obtained from spot profile analysis[22] are fully consistent with the interpretation of a crossover to the exponents of a weak first-order phase transition, for which $\alpha=1$ and $\nu=0.5$ are expected.[33] Therefore, the transition itself must be first order.

In context with our own previous results,[22] the critical exponent α determined by the integrated intensities not only complements our previous data, but corroborates our previous interpretation. Using scaling equations, it even quantitatively fits to our previous data and strengthens the identifi-

cation of the order-disorder transition of this structure as being weakly first order even more. Since we used two different crystals for the present and the previous results, which were of different origin and had different step densities on the surface, these results do not seem to be influenced by small deviations of the surface properties such as step densitities or remaining amounts of impurities on the surface due to the bulk material. All our results are ''consistently'' at variance with those obtained in Ref. 31, where a value of $\alpha = 0.70 \pm 0.04$ is reported. This points towards a systematic difference or error in the data evaluation. A possible reason for the discrepancy might be found in the abnormally low Debye temperature (160 K compared to 280 K in our evaluation) used in Ref. 31. The corresponding large Debye correction of intensities tends to lower all effective critical exponents below T_c, but to increase those above T_c. However, whether full agreement could be reached by proper adjustments of the Debye correction alone is still an open question.

2. H/Ni(111): change of critical exponents by oxygen impurities

For the pure system, we have shown recently that the (2×2)-2H structure on Ni(111) undergoes a continuous order-disorder phase transition with critical exponents belonging to the four-state Potts universality class[32,17] by explicitly determining the critical exponents β, γ, and ν. The critical properties of this system, however, are sensitive to impurities on the surface. We have explicitly investigated the influence of preadsorbed small amounts of atomic oxygen, which under our experimental conditions do not react with the coadsorbed hydrogen.[17] These impurities are not ordered, and, due to their high binding energy to the surface, can be regarded as random frozen defects on the surface close to the critical temperature of the order-disorder transition of the hydrogen layer. We found that whenever the correlation length of critical fluctuations exceeded the average distance between the oxygen atoms, the critical exponents of the pure system were modified, but short-range correlations much larger than this distance still prevail above T_c. The crossover point can be tuned by the average concentration of impurities. In the temperature range influenced by impurities we found critical exponents close to those of the Ising universality class.[34] This result at present is not fully understood. It is unclear whether the effective exponents obtained are true Ising exponents. Even more puzzling, these results contradict the theoretical prediction that arbitrarily small random fields, caused inevitably by adsorbed impurities, should turn the transition to first order.[35] Analytical and simulational results[36] obtained recently, however, show that for weak random fields a system might, in principle, undergo a first-order phase transition in the thermodynamic limit, but system sizes needed to turn the transition to first order are many orders of magnitude larger than those obtainable at present on real surfaces, since this behavior depends only on terms $\propto \ln(L)$, where L is the system size. On finite-size systems that can be studied experimentally, however, the system remains long range ordered up to the system size, and the phase transition appears to be continuous.

Nevertheless, it is still interesting to see whether the effective exponents determined experimentally really coincide with those of the Ising class. For the Ising class, the critical exponent α is zero, and the specific heat should diverge logarithmically ($c \propto -\ln|t|$). We have performed experiments with integrated superstructure beam intensities below T_c analogous to those described above for the other systems. For each amount of preadsorbed oxygen, T_c had to be determined, since the critical temperature shifts linearly with oxygen concentration.[29] From the log-log plots of I' shown in Fig. 10 it can be seen that, apart from finite-size effects below $|t| = 0.007$, deviations from a power law, which corresponds to $\alpha = 0.68 \pm 0.04$ start earlier and earlier as a function of the preadsorbed oxygen concentration. The values of $|t|$, where these deviations set in, agree with those obtained in our earlier studies carried out by spot profile analysis.

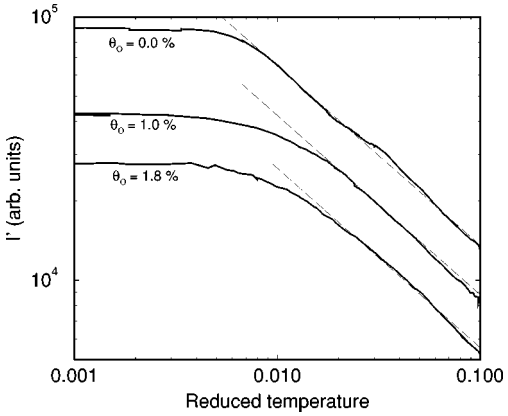

FIG. 10. Derivatives with respect to temperature, I', of (2×2)-2H superstructure spot intensities versus reduced temperature below T_c after the indicated amounts of oxygen were preadsorbed. The dashed lines indicate a power law with the critical exponent $\alpha = 0.68$, which was determined from the oxygen free system.

In order to get more insight we also plotted some of those runs on a semilog scale. Characteristic examples are shown in Fig. 11. These curves exhibit a clear tendency as a function of oxygen concentration to turn the impurity-induced behavior of α towards logarithmic, as indicated by the

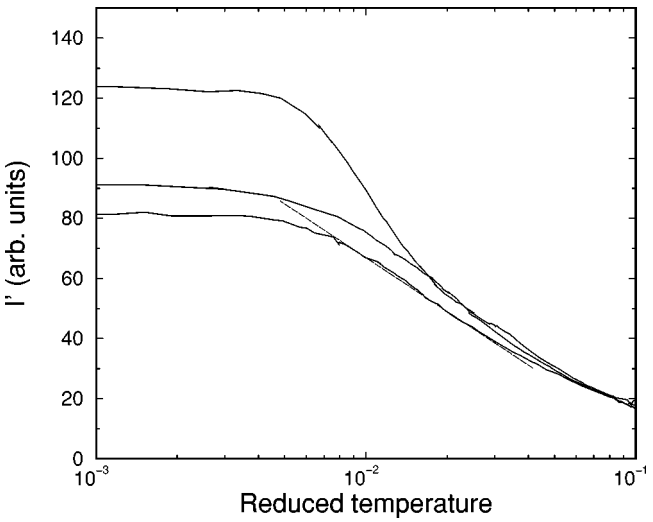

FIG. 11. Semi-log plot of the temperature derivatives of integrated intensities of $(\frac{1}{2}0)$ superstructure spots with 0%, 0.7% and 1.5% ML of oxygen preadsorbed (from top to bottom). Dashed line corresponds to logarithmic behavior. Leveling-off below $t < 0.007$ for all curves is due to finite-size effects.

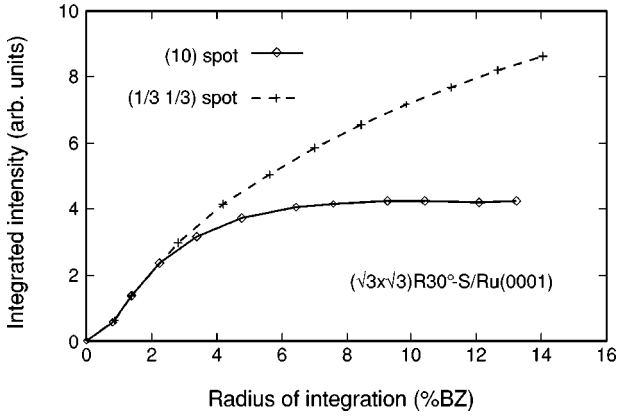

FIG. 12. $(\sqrt{3}\times\sqrt{3})R30°$-S/Ru(0001): Integrated intensities centered at the $k_\parallel$ positions of the $(\frac{1}{3},\frac{1}{3})$ and (1 0) beams, respectively, as a function of the radius of integration. The radii are measured in units of the diameter of the Brillouin zone (BZ). Measuring temperature was 400 K.

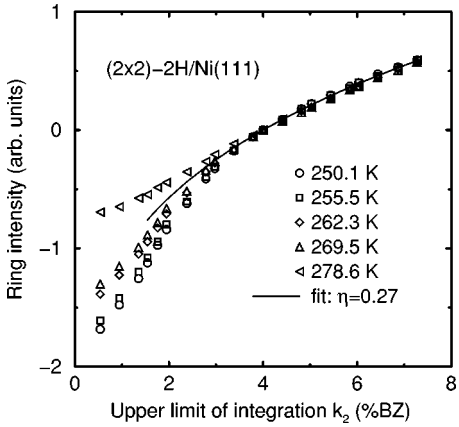

FIG. 13. Integrated ring intensities as a function of $\Delta k_\parallel$, measured in units of the elementary substrate reciprocal-lattice vector, for the system (2×2)-H/Ni(111), and for the temperatures indicated. Note that data were taken both below and above T_c (T_c $=268.2$ K). No rescaling of the data was carried out, but the ring intensity at 3.8% BZ was arbitrarily set to 0 for each run. Line: Fit to a power law according to Eq. (2). For the fit, only data above 3.5% BZ were used.

dashed line in this figure, although we admit that the perfection of the surface used does not allow to uniquely determine a logarithmic dependence. Nevertheless, these investigations demonstrate the sensitivity of the method to impurities. The results obtained are fully compatible with our results from spot profile analysis, but are limited by the quality of the crystal surfaces used. Investigations on better surfaces are underway.

IV. DETERMINATION OF THE CRITICAL EXPONENT η

As visible, e.g., from Fig. 3, the ''contrast'' of integrated intensities seems to saturate for large radii of integration, i.e., the apparent further increase at large K_I is only due to a structureless background. This is in agreement with Eq. (1), which contains a temperature-independent leading term for large $k_\parallel$. At present stage, it is totally unknown whether this limit can be reached experimentally, and at what values of $k_\parallel$. If the leading term of Eq. (1) is dominant, Eq. (2) provides an easy way first of all to test the temperature independence of the integrated ring intensities, and—if this turns out to be true—to quantitatively determine the critical exponent η from fits of the ring intensities as a function of K_I.

The increment of integrated intensities at large $k_\parallel$ is mainly sensitive to short range correlations close to T_c. This property is nicely demonstrated in Fig. 12. It shows examples of integrated intensities for an integer and a fractional order spot. Background has been subtracted by the same procedures as described above, and is assumed to be independent of $k_\parallel$. Whereas the intensity of integer order spots saturates as a function of K_I at a $k_\parallel$ value which is mainly determined by the instrument, the integrated intensity of superstructure spots does not saturate. This behavior can be well explained by the experimentally corroborated fact that $(\sqrt{3}\times\sqrt{3})R30°$-S/Ru(0001) behaves as a lattice gas on well defined threefold-coordinated sites below T_c (Ref. 25)—the measurements were in fact carried out 16 K below T_c. Therefore, the (1×1) coordination measured near the integer order beams is still almost perfectly maintained, and leads to negligible background there. The steady increase of intensity as a function of $k_\parallel$ close to fractional order positions, on the other hand, is due to short-range order $\sqrt{3}$ correlations, and is a direct manifestation of critical scattering below T_c. Since critical scattering below T_c is generally much smaller than above T_c (see, e.g., simulations by Bartelt *et al.*[9]) it is in general not detectable by spot profile analysis below T_c.

Quantitative tests have been carried out for the systems (2×2)-2H/Ni(111), $(\sqrt{3}\times\sqrt{3})R30°$-S/Ru(0001) and $p(2\times2)$-S/Ru(0001). Since all three systems are well described by a lattice gas, information about critical scattering in the sense just explained is only contained in the intensities around superstructure beams. For this purpose, we integrated ring intensities around superstructure spots excluding the center at constant temperature. Thus, the intensity due to long-range order did not contribute. A background subtraction as described above was carried out before analyzing the data, which, as mentioned contained no adjustable parameters. The circle at 4% BZ was arbitrarily chosen as zero.

We first discuss the results for (2×2) ordered H/Ni(111) because they show the most pronounced features (see Fig. 13). Below $k_\parallel=3\%$, there is significant temperature dependence, but the integrated ring intensities above $k_\parallel=4\%$ show little and no systematic dependence on temperature, as predicted by Eq. (2). The remaining small variations, which turned out not to be systematic, can in fact be attributed to uncertainties in background subtraction, which amount up to 5% of the integrated intensity at the largest radii and the highest temperatures. Therefore, the data can be described by only a $k_\parallel$ dependence, but no temperature dependence above an integration radius of 4% BZ. This is unchanged when going through the order-disorder phase transition at T_c $=268.2$ K. Not even a different scaling factor was needed above and below T_c, as required by Eq. (1). From these data we can conclude that we have reached the large $k_\parallel$ limit already at $k_\parallel=4\%$ BZ. All data sets show the same functional dependence on $k_\parallel$, which can be described by a power law according to Eq. (2).

The same behavior, even up to an integration radius of

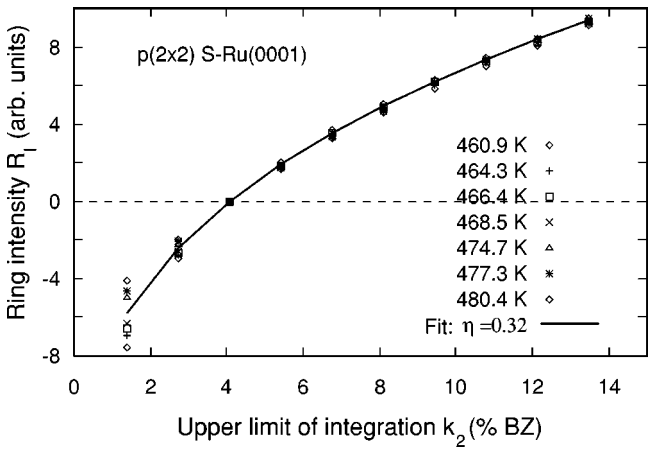

FIG. 14. Integrated ring intensities as a function of $\Delta k_{\parallel}$, for the system $p(2\times2)$-S/Ru(0001), and for the temperatures indicated. Again, data were taken both below and above T_c ($T_c=471.1$ K). Line: Fit to a power law according to Eq. (2).

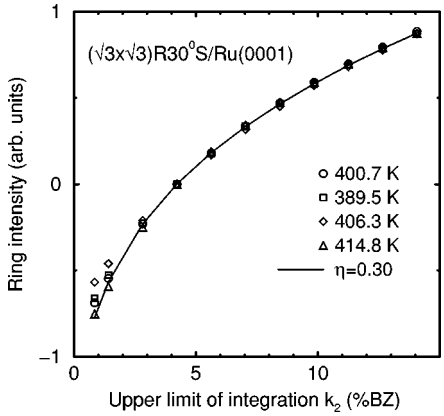

FIG. 15. Integrated ring intensities for the system $\sqrt{3}\times\sqrt{3}R30°$-S/Ru(0001) and fit to determine the critical exponent η. Evaluation analogous to Figs. 13 and 14.

15%, was found for $p(2\times2)$-S/Ru(0001), and is shown in Fig. 14. The limits in $k_{\parallel}$ above which temperature independence and scaling is oberved are very similar to the H/Ni(111) system. Fits to the data according to Eq. (2) were carried out for both systems and for integration radii between 3.5 and 8% for H/Ni and between 3.8 and 15% BZ for $p(2\times2)$-S/Ru(0001). From these fits we determined effective critical exponents $\eta=0.27\pm0.10$ and $\eta=0.32\pm0.10$, respectively. Although the data range is larger for $p(2\times2)$-S/Ru(0001), the uncertainty of η is about the same due to unequal values of the background intensities at different azimuths in the Brillouin zone. This fact increased the uncertainty of background evaluation correspondingly due to the necessary interpolation.

These values for η agree reasonably well with that of the four-state Potts universality class ($\eta_{\text{theor}}=0.25$) to which both order-disorder phase transitions are predicted to belong, if the transitions are continuous.[37] Since also experimentally there is enough evidence which indicates that these transitions are indeed continuous,[7,17] the results for the exponent η presented here are in agreement with expectations. We would like to mention here that, although the precision with which η can be determined is still not as good as for other critical exponents in two-dimensional systems, where the typical precision is around $\pm10\%$, it is much better than that obtained from profile analysis.[7] It would of course be highly desirable to extend the range over which integrated intensities can be measured as a function of $k_{\parallel}$. This does not seem to be feasible. For large $k_{\parallel}$, the physical limit is given by the Brillouin-zone boundary, and we have extended our measurements out as far as possible. (Please note that the units given in Figs. 13, and 14 are with respect to the *substrate* Brillouin zone.) In addition, the signal to background ratio is a major source of uncertainty at large $k_{\parallel}$.

In order to demonstrate that this method of determining the critical exponent η also works for other universality classes, we collected data for the system $(\sqrt{3}\times\sqrt{3})R30°$-S/Ru(0001), which are shown in Fig. 15. Here we obtained an average value $\eta=0.30\pm0.08$. Also this value agrees within error bars very well with that expected from theory ($\eta=0.27$ for three-state Potts systems).

Theory is also corroborated in another aspect: For a continuous phase transition, the ratio of amplitudes A_+/A_- of the leading terms of Eqs. (1) and (2) is expected to be 1, since it does not depend on temperature.[13] In addition, any deviation of this ratio from 1 would cause a jump of the energy at T_c and thus would turn the transition to first order. Experimentally, we find that $A_+/A_-=1\pm0.15$ for all three systems, which again is in full agreement with the theoretical expectations.

This excellent agreement between experiment and theoretical predictions shows that the limit of large $k_{\parallel}\xi$ can be reached rather easily in experimental systems. It is worth noting that much higher uncertainties for η than in our experimental study were estimated in simulations of the structure factor of lattice gas systems with ordered $p(2\times2)$ and $\sqrt{3}\times\sqrt{3}$R30° structures, carried out by Bartelt *et al.*[38] While the origin of this discrepancy cannot be clarified with certainty, finite-size effects may have an influence on the effective values of η in these simulations, especially at small $k_{\parallel}$, since they were carried out on comparatively small systems. Contrary to the simulations just mentioned, we were able to directly demonstrate that critical scattering in this limit is dominated by a term which is independent of temperature. By explicit determination of η we also show that the $k_{\parallel}$ dependence is fully compatible with that given by Eq. (1).

V. CONCLUSIONS

We have experimentally shown that at continuous order-disorder phase transitions in two-dimensional lattice gas systems belonging to the three- and four-state Potts universality classes the limit of large $k_{\parallel}\xi$ is reached above T_c already for values of $k_{\parallel}\xi$ between 2 and 3, whereas below T_c these values are considerably smaller. As a consequence, the successful determination of the critical exponent of the specific heat, α, is possible below T_c even rather far away from the critical temperature, but (small) crossover effects to $(2\beta-1)$ behavior are detectable.

We see no principal problem for the same determination above T_c, but due to the different properties of the scaling function below and above T_c, samples with at least one order of magnitude larger terraces than those used in our experiments would be necessary in order to reach the limit of

large $k_{\parallel}\xi$ over a reasonably wide range of t, since the finite terrace widths limit long-range order in the systems investigated.[7,17]

Although more detailed tests still have to be carried out, this method seems to be able to add valuable information also for systems the critical properties of which are not yet fully understood. We have investigated as examples O/Ni(111)-$p(2\times2)$, which exhibits a weak first-order phase transition, and the impurity-induced effects in the system (2×2)-2H/Ni(111).

The analysis of the $k_{\parallel}$ dependence of integrated intensities shows that critical scattering is observable quantitatively and directly also below T_c. The limit where a term dominates which depends only on $k_{\parallel}$, but not on temperature, can be reached rather easily. This finding at first sight seems to contradict the fact that the amplitude of critical scattering is much smaller below T_c compared to that above T_c, but this argument is only valid for small $k_{\parallel}\xi$.

We would like to mention at the end that all our observations were carried out with an instrument with a transfer width of approximately only 100 Å. Nevertheless, we observed influences on the correlation length on a much larger length scale, such as finite size effects, influences by impurities, etc. These results are demonstrations that, close to continuous phase transitions, fluctuations occur on all length scales. Correspondingly, the properties of the fluctuations change on all scales once the properties of the system, seen by the most relevant quantity, the correlation length, are altered. These changes can be most easily recorded by integrated intensities in a diffraction experiment.

ACKNOWLEDGMENTS

This work was supported by the Deutsche Forschungsgemeinschaft. Useful discussions with I. Lyuksyutov are gratefully acknowledged.

[1] B.N.J. Persson, Surf. Sci. Rep. **15**, 1 (1992).
[2] E. Bauer, in *Structure and Dynamics of Surfaces II*, edited by W. Schommers and P. von Blanckenhagen, Topics in Current Physics, Vol. 43 (Springer, Berlin, 1987), p. 115.
[3] T. L. Einstein, in *Chemistry and Physics of Solid Surfaces VII*, edited by R. Vanselow and R. Howe (Springer, Berlin, 1988), p. 307.
[4] B. Shalaev, Phys. Rep. **23**, 131 (1994).
[5] P. Piercy and H. Pfnür, Phys. Rev. Lett. **59**, 1124 (1987).
[6] M. Sokolowski and H. Pfnür, Phys. Rev. Lett. **63**, 183 (1989).
[7] M. Sokolowski and H. Pfnür, Phys. Rev. B **49**, 7716 (1994).
[8] Y. Nakajima, C. Voges, T. Nagao, S. Hasegawa, G. Klos, and P. Pfnür, Phys. Rev. B **55**, 8129 (1997).
[9] N.C. Bartelt, T.L. Einstein, and L.D. Roelofs, Phys. Rev. B **32**, 2993 (1985).
[10] P. Pfnür and P. Piercy, Phys. Rev. B **40**, 2515 (1989).
[11] W.N. Unertl, Comments Condens. Matter Phys. **12**, 289 (1986).
[12] N.C. Bartelt, T.L. Einstin, and L.D. Roelofs, Surf. Sci. **149**, L47 (1985).
[13] M.E. Fisher, Rev. Mod. Phys. **46**, 597 (1974).
[14] J.M. Kosterlitz and D.J. Thouless, J. Phys. C **60**, 1181 (1973).
[15] D.R. Nelson and B.I. Halperin, Phys. Rev. B **19**, 2457 (1979); A.P. Young, *ibid.* **19**, 1855 (1979).
[16] P.A. Heiney, P.W. Stephens, R.J. Birgeneau, P.M. Horn, and D.E. Moncton, Phys. Rev. B **28**, 6416 (1983).
[17] K. Budde, L. Schwenger, C. Voges, and H. Pfnür, Phys. Rev. B **52**, 9275 (1995).
[18] C. Voges and H. Pfnür, Europhys. Lett. **38**, 165 (1997).
[19] M.E. Fisher, Phys. Rev. **176**, 257 (1968).
[20] V. Zielasek, A. Büssenschütt, and M. Henzler, Phys. Rev. B **55**, 5398 (1997).
[21] L.N. Babanskaya, M.A. Valisev, and S.D. Gorodetskii, Phys. Metals **5**, 481 (1985).
[22] L. Schwenger, C. Voges, M. Sokolowski, and H. Pfnür, Surf. Sci. **307-309**, 781 (1994).
[23] C. Schwennicke, D. Jürgens, G. Held, and H. Pfnür, Surf. Sci. **316**, 87 (1994).
[24] W. Ho, N.J. DiNardo, and E.W. Plummer, J. Vac. Sci. Technol. **17**, 134 (1980).
[25] C. Schwennicke, M. Sandhoff, W. Sklarek, D. Jürgens, and H. Pfnür, Phys. Rev. B **52**, 2138 (1995).
[26] F.Y. Wu, Rev. Mod. Phys. **54**, 235 (1982).
[27] A.D. Bruce, J. Phys. C **14**, 193 (1981).
[28] C. Tracy and B. McCoy, Phys. Rev. B **12**, 368 (1975).
[29] C. Voges, Ph.D. thesis, Universität Hannover, 1996.
[30] L.D. Roelofs, A.R. Kortan, T.L. Einstein, and R.L. Park, Phys. Rev. Lett. **46**, 1465 (1981).
[31] Z. Li, X. Liang, and R.D. Diehl, Surf. Sci. **327**, 121 (1995).
[32] L. Schwenger, K. Budde, C. Voges, and H. Pfnür, Phys. Rev. Lett. **73**, 296 (1994).
[33] M.E. Fisher and A.N. Berker, Phys. Rev. B **26**, 2507 (1982).
[34] H. Pfnür, C. Voges, K. Budde, and L. Schwenger, Prog. Surf. Sci. **53**, 205 (1996).
[35] W. Kinzel, Phys. Rev. B **27**, 5819 (1983).
[36] I. Lyuksyutov and H. Pfnür (unpublished).
[37] M. Schick, Prog. Surf. Sci. **11**, 245 (1981).
[38] N.C. Bartelt, T.L. Einstein, and L.D. Roelofs, Phys. Rev. B **35**, 1776 (1987).